ASSESSING SURFACE FLOWPATH INTERCEPTION BY VEGETATIVE BUFFERS USING ARCGIS HYDROLOGIC MODELING AND GEOSPATIAL ANALYSIS FOR ROCK CREEK WATERSHED IN CENTRAL IOWA

D. F. Webber, M. Bansal, S. K. Mickelson, M. J. Helmers, K. Arora, B. K. Gelder, M. Shrivastav, C. J. Judge

ABSTRACT. *Nonpoint-source (NPS) pollution is a major cause of surface water quality degradation due to the transport of chemicals, nutrients, and sediments into lakes and streams. Vegetative buffers comprise several effective landscape best management practices (BMPs) that include vegetative filter strips (VFS) and grassed waterways. However, some BMPs are less effective due to concentrated surface flow, improper cropland-to-VFS area ratios, and surface flowpaths that partially or completely bypass vegetative buffers. The overall objective of this study was to quantify the accuracy of simulated flowpaths relative to observed and global positioning system (GPS)-assisted ground-truthed surface flowpaths for improved placement of VFS and other vegetative buffers to effectively intercept surface runoff. This study was conducted on three research sites in Rock Creek watershed in central Iowa. Geographic information system (GIS) software was used for flowpath hydrologic modeling and geospatial map comparison analysis. Digital elevation model (DEM) datasets were used for flowpath simulation and included internet-available USGS 30 m × 30 m grid (typically used to design and site VFS buffers) and light detection and ranging (LiDAR) 5 m × 5 m grid DEMs. Results from this study indicate that the LiDAR 5 m × 5 m DEM generated significantly more accurate simulated flowpaths than the USGS 30 m × 30 m DEM. These results quantitatively underscore the efficacy of using high-resolution LiDAR DEM data to more accurately determine how well surface flowpaths are intercepted by VFS and other vegetative buffers. These results also demonstrate the benefits of coupling high-resolution aerial imagery with quantitative geospatial map comparison data to improve visualization and comparison of field-scale and watershed-scale hydrologic and terrestrial attributes. Ultimately, the results and procedures from this study will be applied to the development of a novel cloud-based, user-interactive, virtual-reality decision support (DS) tool that can be used to remotely assess hydrologic landscape conditions, prescribe improvements to existing BMPs, and determine new sites for enhanced BMP placement and functionality within a high-resolution 3-D imagery environment.*

Keywords*. ArcGIS, Best management practices (BMPs), Decision support (DS) tool, Digital elevation model (DEM), Geospatial analysis, Light detection and ranging (LiDAR), Nonpoint-source (NPS) pollution, Surface runoff, Vegetative filter strip (VFS), Watershed hydrologic modeling.*

Water quality is a significant global issue that is connected to rising concerns about increasing human health hazards and death rates of aquatic organisms. In re-sponse to escalating public awareness of water pollution and its negative effects on the environment, the U.S. Environmental Protection Agency (USEPA) developed criteria for water quality that included the latest scientific knowledge about the effects of pollutants on human health and aquatic life (USEPA, 2000). As a result of this effort, the USEPA identified over 41,000 water bodies nationally that exceeded the water quality standards for maximum pollutant levels (USEPA, 2012). Nonpoint-source (NPS) pollution that results from water movement over and through the land surface significantly contributes to surface water quality degradation (Subra and Waters, 1996). Although the USEPA has been bound since the early 1970s by legislation that addresses only point-source pollution from industrial and municipal sources, NPS pollution is also a major environmental threat due to the transport of nutrients, sediments, and chemicals from agricultural fields into surface water bodies throughout the U.S. (USEPA, 2009; USGS, 2010).

To address the NPS pollution threat, the USDA Natural

Submitted for review in March 2017 as manuscript number NRES 12350; approved for publication as part of the "Advances in Drainage: Selected Works from the 10th International Drainage Symposium" collection by the Natural Resources & Environmental Systems Community of ASABE in October 2017.

The authors are **David F. Webber,** Associate Scientist, Department of Agricultural and Biosystems Engineering, Iowa State University, Ames, Iowa; **Manveen Bansal,** Data Engineer, Amazon.com, Inc., Seattle, Washington; **Steven K. Mickelson,** Professor and Chair, **Matthew J. Helmers,** Dean's Professor, **Kapil Arora,** Field Specialist, **Brian K. Gelder,** Associate Scientist, **Manish Shrivastav,** Graduate Research Assistant, Department of Agricultural and Biosystems Engineering, Iowa State University, Ames, Iowa; **Casey J. Judge,** Graduate Research/Teaching Assistant, Department of Ecology, Evolution, and Organismal Biology, Iowa State University, Ames, Iowa. **Corresponding author:** David Webber, 3354 Elings Hall, Iowa State University, Ames, IA 50011-1098; phone: 515-294-6798; email: davw@iastate.edu.

Vol. 61(1): 273-283 ISSN 2151-0032 https://doi.org/10.13031/trans.12350

Resource and Conservation Service (NRCS) has taken significant steps toward mitigation by designing and implementing various types of vegetative buffers. Vegetative buffers include various landscape best management practices (BMPs), such as grassed waterways and upland and riparian vegetative filter strip (VFS) buffers. A VFS is a BMP that helps reduce surface water transport of nutrients, sediments, and agrochemicals into receiving waters. A typical VFS comprises bands of planted or indigenous vegetation situated downslope from cropland or animal production facilities. This BMP filters nutrients, sediments, organics, pathogens, and pesticides from agricultural runoff before the contaminants reach a water system (Dillaha et al., 1989).

VFS buffers have also been shown to significantly reduce sediment delivery by slowing runoff velocity and filtering sediment (Neibling and Alberts, 1979; Van Dijk et al., 1996). VFS and other vegetative BMPs reduce the movement of suspended material in runoff, such as soil particles and plant residue, and promote settling of the material through sedimentation. Although most of these BMPs have been used effectively for several years to treat surface runoff from agricultural land, some VFS buffers have been found to be less effective due to concentrated surface flow (Meyer et al., 1995; Dosskey et al., 2002), improper cropland-to-VFS area ratios (Dosskey et al., 2011), and surface runoff that partially or completely bypasses the VFS area (Bansal, 2006).

Several studies assessing the effectiveness of VFS in intercepting and treating surface runoff have shown that the efficacy of this BMP is influenced by several factors, including the VFS length and width (Wenger, 1999; Zreig et al., 2004), the ratio of runoff source area to VFS area (Dosskey et al., 2011), the VFS buffer species (Ree, 1949; Broadmeadow and Nisbet, 2004), VFS nutrient and sediment trapping (Meyer et al., 1995; Van Dijk et al., 1996; Gharabhaghi et al., 2001; Zreig, 2001; Lee et al., 2003; Webber et al., 2010a, 2010b), VFS performance (Dosskey et al., 2007), concentrated surface flow (Dosskey et al., 2002), and chemical and nutrient concentrations in runoff (Arora et al., 1996, 2003; Boyd et al., 2003; Webber et al., 2009).

Hydrologic modeling and geospatial map comparison analysis using ArcGIS software and high-resolution light detection and ranging (LiDAR) digital elevation model (DEM) data have been shown to generate accurate surface flowpath networks and drainage areas (NSSDA, 1998; Murphy et al., 2008; Zhao et al., 2010; Vaze et al., 2010; Shrivastav, 2015). Moreover, several studies have further applied and evaluated LiDAR DEM data for improving the results from modeling low-relief and depression topography, determining the effects of various DEM sources on hydrologic applications, and rectifying errors associated with DEM interpolation (Jones et al., 2008; Liu, 2008; Zhang and Huang, 2009; Bater and Coops, 2009; Li and Wong, 2010; Li et al., 2011). Consequently, the new LiDAR DEM should generate better simulated flowpath network data versus the earlier lower-resolution USGS DEM for improved VFS landscape placement to more effectively intercept surface runoff flow from contributing source areas.

Research by Minnick (1964), Unwin (1981), Goodchild and Hunter (1997), Webber (2000), Bansal (2006), and Shrivastav (2015) contributed to developing manual and automated GIS hydrologic modeling and geospatial map comparison analysis procedures for comparing observed and simulated surface and subsurface flowpaths and watershed boundaries derived from paper topographic map data and USGS 30 m × 30 m and LiDAR 5 m × 5 m DEMs. The USGS 30 m × 30 m DEM data have been used for approximately 20 years by NRCS personnel to design and place VFS buffers and other BMPs, and this DEM continues to be used by the NRCS in the new Land Management Operations Database (LMOD) environmental landscape data referencing system (David et al., 2014).

The overall objective of this study was to quantify the accuracy of simulated surface flowpaths relative to observed and ground-truthed BMP drainage features for three selected Rock Creek watershed research sites to improve the placement of VFS and other vegetative buffer practices for intercepting surface runoff. This study used the internet-available USGS 7.5 min quadrangle map-derived 30 m × 30 m National Elevation Database (NED) DEM (typically used for designing and siting VFS buffers) and the airborne sensor-derived LiDAR 1 m × 1 m DEM (Wehr and Lohr, 1999; Shrivastav, 2015). To process and analyze these DEM datasets, GIS hydrologic modeling functions and geospatial map comparison analysis procedures were used. The resampled 5 m × 5 m LiDAR DEM data were used versus the original 1 m × 1 m LiDAR DEM to initially minimize the elevation dataset file size and possibly boost the computer processing efficiency. However, it was statistically determined that the file size differences for the USGS 30 m × 30 m and LiDAR 5 m × 5 m DEM data were insignificant ($p = 0.387$ at 95% probability level [$p \leq 0.05$]).

Specific short-term and long-term objectives of this research effort included:

- Generating simulated surface flowpaths and vegetative buffer features using ArcGIS hydrologic modeling functions and USGS 30 m × 30 m and LiDAR 5 m × 5 m DEM datasets for three research sites in Rock Creek watershed in central Iowa.
- Determining actual surface flowpath networks, contributing runoff areas, and vegetative buffer locations using detailed on-site field observations, GPS-assisted ground-truthing procedures, and high-resolution aerial imagery.
- Comparing simulated surface flowpaths to actual ground-truthed flowpaths and vegetative buffers using ArcGIS geospatial map comparison analysis tools and statistical analysis methods.
- Applying these findings and procedures to a current research effort using additional central Iowa research watersheds for developing a novel cloud-based, user-interactive, virtual-reality decision support (DS) tool for field-scale and watershed-scale hydrologic assessment and vegetative BMP design and placement within a high-resolution 3-D imagery environment.

Materials and Methods

Field Research Sites and Soil Types

The initial and final phases of this study were conducted during 2004-2006 (Bansal, 2006) and 2013-2015 (Shrivastav, 2015), respectively. These field and laboratory efforts used detailed on-site observations, GPS-assisted ground-truthing methods, and GIS-based hydrologic data, DEM data, geospatial map comparison analysis, and high-resolution aerial imagery for three agricultural field research sites in Rock Creek watershed (fig. 1), located in northeastern Jasper County and southeastern Marshall County in central Iowa (41° 46.21′ N, 95° 50.33′ W). This watershed drains into Rock Creek Lake, which is adjacent to a large campground that offers residents of central Iowa a range of recreational opportunities. However, the water quality of Rock Creek Lake has been at risk due to sediment and nutrient transport from agricultural fields to the streams that drain into the lake.

This watershed-level hydrologic study included three row crop research sites in Jasper County from which agricultural runoff is contributing to the water quality of Rock Creek Lake. Each of these three sites contained multiple sub-basin field areas. These fields were primarily established as two-year crop rotations of corn (*Zea mays* L.) and soybean (*Glycine max* L.). Transport of sediment and chemicals from these fields is suspected to have led to algal blooms in Rock Creek Lake, resulting in low levels of oxygen that have affected the water quality and aquatic biodiversity. The research sites are identified as sites 1, 2, and 3 and were selected for this study based on the presence of established vegetative buffers and other conservation BMPs. The VFS buffers were designed by NRCS personnel primarily to reduce the transport of nutrients, pesticides, and sediment in runoff from the cropland source areas. Table 1 includes the soil types and descriptive information for the three research sites.

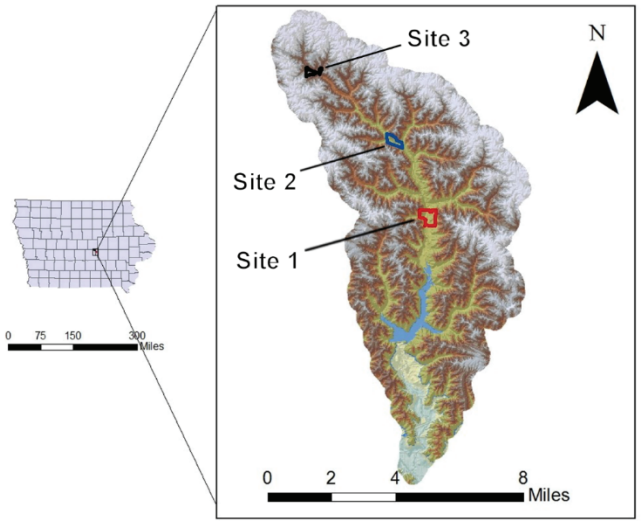

Figure 1. Rock Creek watershed location, boundary, stream network, and three research sites that each included multiple sub-basin field areas in Jasper County, Iowa.

Site 1 (figs. 3 and 4) included a stream, running through the center of the site, that flowed into Rock Creek Lake. The approximately 35 m wide VFS buffers were installed in 2000 by the landowner on both sides of the stream immediately downslope from the cropland runoff source area, which was in a corn-soybean rotation. Site 1 also had terraces and grassed waterways that divided the site into three sub-basin field areas: 1A, 1B, and 1C (figs. 3 and 4).

Visual observations and in-field surveying of areas 1A and 1B indicated that only a small portion of the surface runoff flowed through the riparian VFS buffers. Observed undulations in area 1A caused surface runoff to bypass the VFS area and flow toward the natural riparian area south of the sub-basin area instead of flowing through the VFS. Traces of sedimentation at the leading edge of the VFS were observed, indicating that runoff reached the VFS after rainfall events. However, from topographic observations, this would have been possible only in cases of significantly heavy rainfall.

Site 2 (figs. 5 and 6) was located north of site 1 and also included a stream running through the site. The stream had approximately 18 m wide VFS buffers on both sides. Although surface runoff entering the VFS was evident from visual observations at this site in 2004, figure 6 shows considerable circumvention of the VFS areas from the ground-truthed and verified simulated flowpaths. The adjacent cropped fields used no-till conservation practices. A gully was found in the southeastern part of the field. Deer paths were also noted at the leading edge of the VFS, indicating that wildlife activity may have exacerbated the concentrated surface flow conditions. This field was divided into two sub-basin field areas (2A and 2B) with a VFS on each side of the stream.

Site 3 (figs. 7 and 8) was located in the extreme northern headwaters region of Rock Creek watershed and originally included 30 m wide VFS buffers on both sides of the stream and six 18 m wide grassed waterways that were observed in 2004. However, by 2014, the riparian VFS on the north side of Rock Creek had been eliminated, and only a narrow remnant VFS remained on the south side of the stream and three grassed waterways remained in the general site area. Site 3 also included three sub-basin field areas: 3A, 3B, and 3C. The presence of a draw divided site 3 into areas 3A and 3B. The adjacent field areas were planted to corn in 2006. Area 3C was located on the northeastern side of site 3, where it originally included an 18 m wide grassed waterway. However, that grassed waterway had been eliminated by 2014.

Surface Flowpath Network Delineation

Computer software that comprised GIS hydrologic modeling functions and geospatial analysis utilities was used for delineating the positions of stream networks and drainage area boundaries and for locating drainage outlet points in the field. During the initial research phase (Bansal, 2006), these

Table 1. Dominant soil type, description, and physical properties at Rock Creek watershed sites 1, 2, and 3 (Nestrud and Worster, 1979).

Site	Soil Series	Soil Description	Bulk Density ($g\ cm^{-3}$)	Clay (%)	Permeability ($cm\ h^{-1}$)
1	Tama	Fine-silty, mixed, mesic Typic Argiudolls	1.40	18 to 26	1.5 to 5.1
2	Ackmore	Fine-silty, mixed, mesic Aeric Fluvaquents	1.35	28 to 32	1.5 to 5.1
3	Ackmore-Colo complex	Fine-silty, mixed, mesic Aeric Fluvaquents; Fine-silty, mixed, mesic Cumulic Haplaquolls	1.35	20 to 26	1.5 to 5.1

GIS software programs included ArcGIS 9.3, ArcView (AV) 3.3, AV Soil and Water Assessment Tool (AVSWAT), and AV Spatial Analyst extensions (ESRI, 2005). ArcGIS 10.3 and 10.4 (ESRI, 2014, 2016) were used during the final phase (Shrivastav, 2015).

The topographic surfaces of the three research sites were represented by regularly gridded DEM datasets. In this study, USGS 30 m × 30 m DEM data were used to identify sinks in the field site drainage areas and generate watershed flow accumulation, outlets, and stream network and drainage basin areas in ArcGIS 9.3. During the final phase, LiDAR 5 m × 5 m DEM data were used to obtain simulated hydrologic surface flowpaths and drainage features in ArcGIS 10.3 and 10.4. Automatic and manual drainage area delineation procedures were used to produce GIS layers of the contributing drainage areas for comparison with the observed and GPS-assisted ground-truthed boundary locations.

Drainage Feature Observations and Ground-Truthing Surveys

On-site observations and GPS ground-truthing surveys for sites 1, 2, and 3 were initially conducted in 2005 using a Trimble 5800-R8 (Trimble, 2005) handheld GPS unit (Bansal, 2006). The final phase of on-site observations and ground-truthing surveys was conducted in 2013 and 2014 using Magellan SporTrak Map and Explorist 200 (Magellan, 2004) handheld GPS units (Shrivastav, 2015). Because these GPS units are consumer-grade and are considered less accurate than survey-grade GPS units, both of the Magellan GPS units were used simultaneously during the final phase for cross-checking position coordinates. After averaging the GPS coordinate data from these two units, it was determined in the laboratory that the two Magellan units provided mostly sub-meter position accuracy, with GPS points located generally within 10 to 20 cm of the actual points and linear drainage features observed in the field. Eventually, the surveys provided the positions of twelve 100 m long ground-truthed flowpaths distributed among the three study sites.

Hydrologic Geospatial Map Comparison Analysis

The numerical basis for the hydrologic geospatial map comparison analysis used to evaluate the accuracy of the simulated flowpath network relative to the on-site GPS ground-truthed and verified drainage feature positions was derived from a coefficient of areal correspondence (CAC) map comparison approach. This approach was developed and further described by Minnick (1964) and Unwin (1981), respectively. A linear-based geospatial map comparison equation was used by Goodchild and Hunter (1997) to simulate ocean shoreline features, and the approach was further adapted by Webber (2000) to simulate subsurface tile drain locations from DEM and stream channel map data for a central Iowa watershed. For this study, the coefficient of linear correspondence (CLC) approach was adapted (eq. 1):

$$CLC = \frac{\text{Total simulated flowpath length (m) within 5 m buffer of observed flowpath segment}}{\text{Observed and ground-truthed 100 m flowpath segment}} \quad (1)$$

The CLC equation (eq. 1) divides the total simulated flowpath length (m) that falls within the designated 5 m buffer area around the selected 100 m long observed and ground-truthed flowpath segment by the observed 100 m flowpath length. The 5 m buffer distance used for calculating the CLC values was chosen primarily because it equals the highest resolution value of the LiDAR 5 m × 5 m DEM versus the USGS 30 m × 30 m DEM. Similar to the CAC equation, the CLC equation (eq. 1) generates a coefficient that is expressed as a dimensionless decimal value from 0.0 to 1.0 (0.0 = low; 1.0 = high). Figure 2 illustrates the CLC equation applied to actual observed and

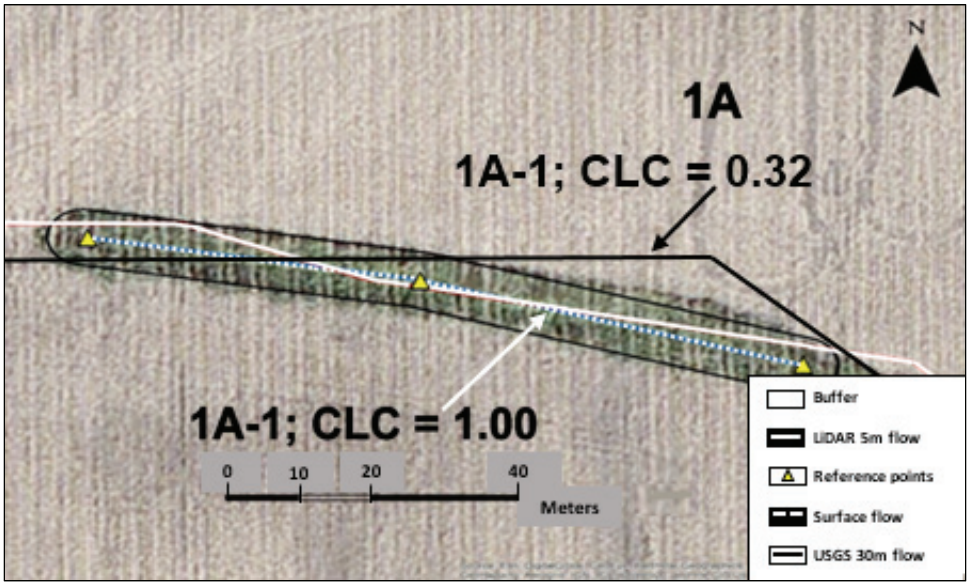

Figure 2. Sub-basin area 1A of site 1 (fig. 4) grassed waterway (darker area) with LiDAR 5 m × 5 m DEM flowpath (solid white line), USGS 30 m × 30 m DEM flowpath (solid black line), ground-truthed reference points (yellow triangles), observed 100 m flowpath segment (dashed white line), and 5 m wide buffer area (gray outline) for calculating the unitless coefficient of linear correspondence (CLC) with equation 1. The geospatial map comparison analysis results given here for the USGS DEM (CLC = 0.32; black arrow) and the LiDAR DEM (CLC = 1.00; white arrow) are given for the other sites in Rock Creek watershed in figures 3 through 8.

Table 2. Performance ratings for percent bias (PBIAS) values for flowpath length (adapted from Moriasi et al., 2007, and Starks and Moriasi, 2017).

Performance Rating	PBIAS (%)
Very good	PBIAS < ±10
Good	±10 ≤ PBIAS < ±15
Satisfactory	±15 ≤ PBIAS < ±25
Unsatisfactory	PBIAS ≥ ±25

simulated flowpaths for conducting a hydrologic geospatial map comparison of a surface drainage feature in sub-basin area 1A of site 1.

Statistical Analysis and Model Performance

Statistical analysis of the mean values of simulated flowpath length was performed using SAS version 9.4 (SAS, 2016). Significant differences and coefficients of variation (CV) among the simulated USGS 30 m × 30 m and LiDAR 5 m × 5 m DEM data-generated mean values of flowpath length (occurring within 5 m buffer areas around the observed 100 m flowpath segments) were determined by applying the SAS general linear model (GLM), analysis of variance (ANOVA), and least square means (LSMEANS) procedures at the 5% probability level ($p \leq 0.05$). An additional statistical metric used in this study was percent bias (PBIAS) for flowpath length, with general performance ratings (table 2) adapted from Moriasi et al. (2007) and Starks and Moriasi (2017). Due to the complex flowpath and buffer area annotations on the site maps in figures 3 through 8, the twelve observed and ground-truthed 100 m surface flowpaths shown in the oval outlines are also designated as LiDAR 5 m × 5 m DEM-generated flowpaths within oval outlines in figures 4, 6, and 8. This approach was taken because the GPS-surveyed locations of the simulated 5 m × 5 m LiDAR flowpaths (with generally sub-meter accuracy) were extremely close and would be difficult to resolve from the observed and verified 100 m flowpath segments.

Results and Discussion

Hydrologic Geospatial Analysis of Surface Flowpath Network

Table 3 lists the observed 100 m flowpath segment lengths, average simulated flowpath lengths, and site average flowpath lengths for Rock Creek watershed sites 1, 2, and 3. In addition to the average flowpath lengths and CLC values, table 3 lists the statistical analysis results, including significant means of flowpath length and CLC as indicated by different letters ($p \leq 0.05$). Table 4 shows the PBIAS values for flowpath length based on the general performance ratings (table 2).

Figures 3 and 4 show the hydrologic modeling and geospatial map comparison analysis results for Rock Creek watershed site 1. The oval outlines identify four observed and ground-truthed 100 m long flowpath segments and their respective CLC values (1A-1, 1A-2, 1B-1, and 1C-1). Table 3 lists the average flowpath lengths (m) and CLC values for the USGS 30 m × 30 m and LiDAR 5 m × 5 m DEMs. These results indicate significantly lower ($p \leq 0.05$) total lengths for the USGS 30 m × 30 m DEM-derived flowpaths that occur within the observed 5 m wide buffered 100 m flowpath segments (in the oval outlines). However, the results for the LiDAR 5 m × 5 m DEM-derived flowpaths, compared with the observed 5 m buffered 100 m flowpath segments, indicate no significant differences ($p \leq 0.05$) and highly accurate simulated flowpaths.

Table 3. Surface flowpath geospatial map comparison and ANOVA results for Rock Creek watershed sites 1, 2, and 3. Results include observed 100 m flowpath and equivalent 1.00 CLC values for comparison of USGS 30 m × 30 m and LiDAR 5 m × 5 m DEMs, mean simulated flowpath lengths occurring within 5 m buffer width, and CLC values for USGS 30 m × 30 m and LiDAR 5 m × 5 m DEMs. Means followed by different letters are significantly different ($p \leq 0.05$).

		Simulated Flowpath Length (m) within 5 m Buffer Width		CLC Value (unitless)	
Site	Observed Flowpath / CLC	USGS 30 m DEM	LiDAR 5 m DEM	USGS 30 m DEM	LiDAR 5 m DEM
1	100 a / 1.00 a	14.50 b	100.0 a	0.15 b	1.00 a
2	100 a / 1.00 a	25.50 b	97.25 a	0.26 b	0.97 a
3	100 a / 1.00 a	19.25 b	98.00 a	0.20 b	0.98 a

Table 4. Surface flowpath geospatial map comparison analysis for Rock Creek watershed sites 1, 2, and 3 in central Iowa. Results include percent bias (PBIAS) values for simulated flowpath lengths occurring within 5 m buffer width of observed 100 m flowpath segments for 30 m × 30 m USGS and 5 m × 5 m LiDAR DEMs.

	PBIAS (%) for Simulated Flowpath Lengths Occurring within 5 m Buffer Width	
Site	USGS 30 m DEM	LiDAR 5 m DEM
1	85.50	0.00
2	74.50	2.75
3	80.75	2.00

The USGS 30 m × 30 m DEM-derived flowpaths that are oriented perpendicularly through the riparian VFS in the northwest area (1A in fig. 3) give the false appearance of effective flowpath interception by the VFS buffer. While this generally inaccurate simulated flowpath pattern has been referred to as "corrugated," such errant flowpath directions have commonly been attributed to 30 m × 30 m or lower resolution DEM data applied to low-relief areas (similar to central Iowa) (Webber, 2000). This DEM resolution issue generally occurs when the raster or grid cell size and elevation intervals are too large to correctly render certain horizontal and vertical changes in the landscape (Wang and Yin, 1998; Richardson and Gatti, 1999; Webber, 2000).

Conversely, the LiDAR 5 m × 5 m DEM-derived flowpath network in the same area (1A in fig. 4) indicates that a ground-truthed and verified flowpath runs parallel to the stream channel, completely bypassing the riparian VFS area. Ground-truthed flowpaths also partially bypass the VFS buffers in areas 1B and 1C (fig. 4). These simulated flowpath patterns relative to the vegetative conservation BMP areas present a case in which high-resolution LiDAR DEM data and aerial imagery can be applied to precisely place vegetative buffers to effectively intercept surface runoff. A potentially significant implication is that there could be many more locations in central Iowa where surface flow bypasses vegetative buffers because the NRCS had used lower-resolution USGS DEM data to design and place vegetative buffers since about 1997.

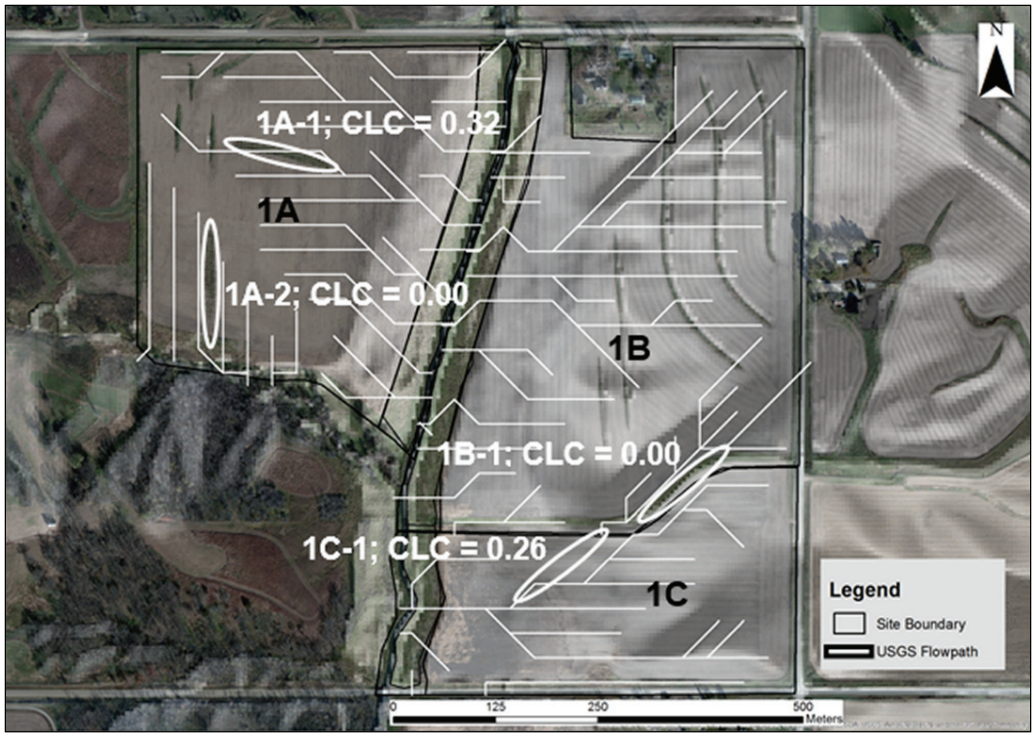

Figure 3. Sub-basin field areas 1A, 1B, and 1C of site 1 showing USGS 30 m × 30 m DEM-derived flowpaths, observed 100 m flowpath segments (ovals), and coefficients of linear correspondence (CLC) based on geospatial map comparison analysis for Rock Creek watershed in central Iowa.

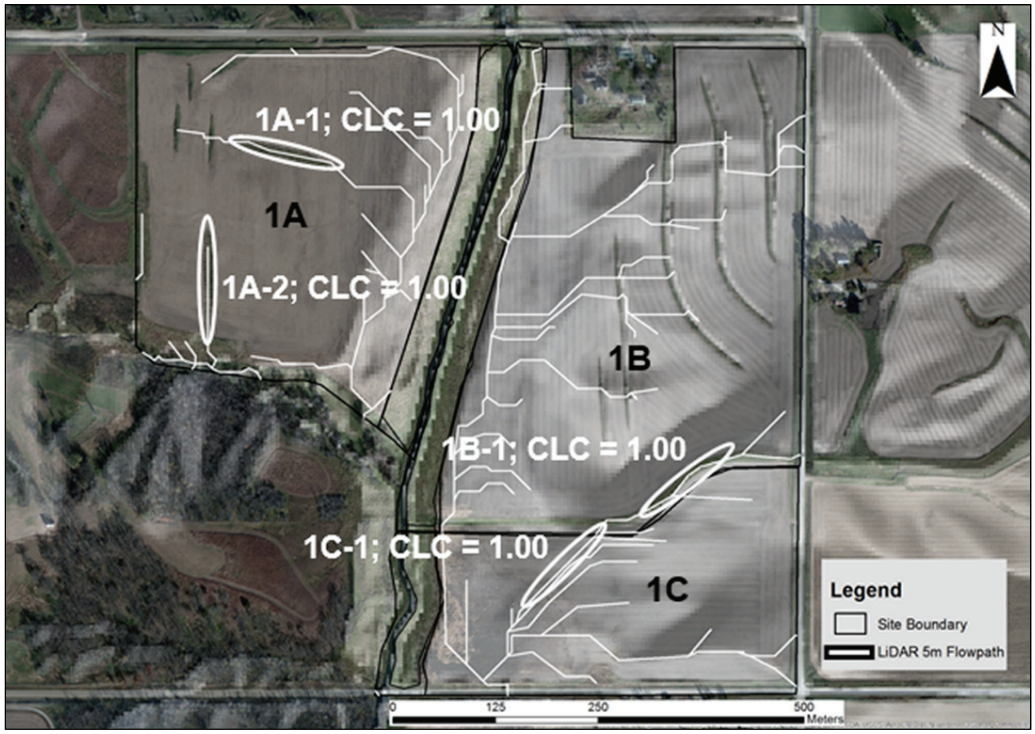

Figure 4. Sub-basin field areas 1A, 1B, and 1C of site 1 showing LiDAR 5 m × 5 m DEM-derived flowpaths, observed 100 m flowpath segments (ovals), and coefficients of linear correspondence (CLC) based on geospatial map comparison analysis for Rock Creek watershed in central Iowa.

A plausible improvement scenario for area 1A could include extending the present riparian VFS area away from the stream channel to include the targeted flowpath. An alternative scenario might involve two narrow (10 m) VFS buffers that include the targeted flowpath and are also adjacent to the stream channel to help maintain the integrity of the field edge and streambank. Although NRCS programs currently do not support a variable-width buffer option, this conservation practice has received some attention as an alternative BMP. With dynamic crop production economics almost certain, variable-width buffers could allow producers to increase crop production areas while maintaining effective

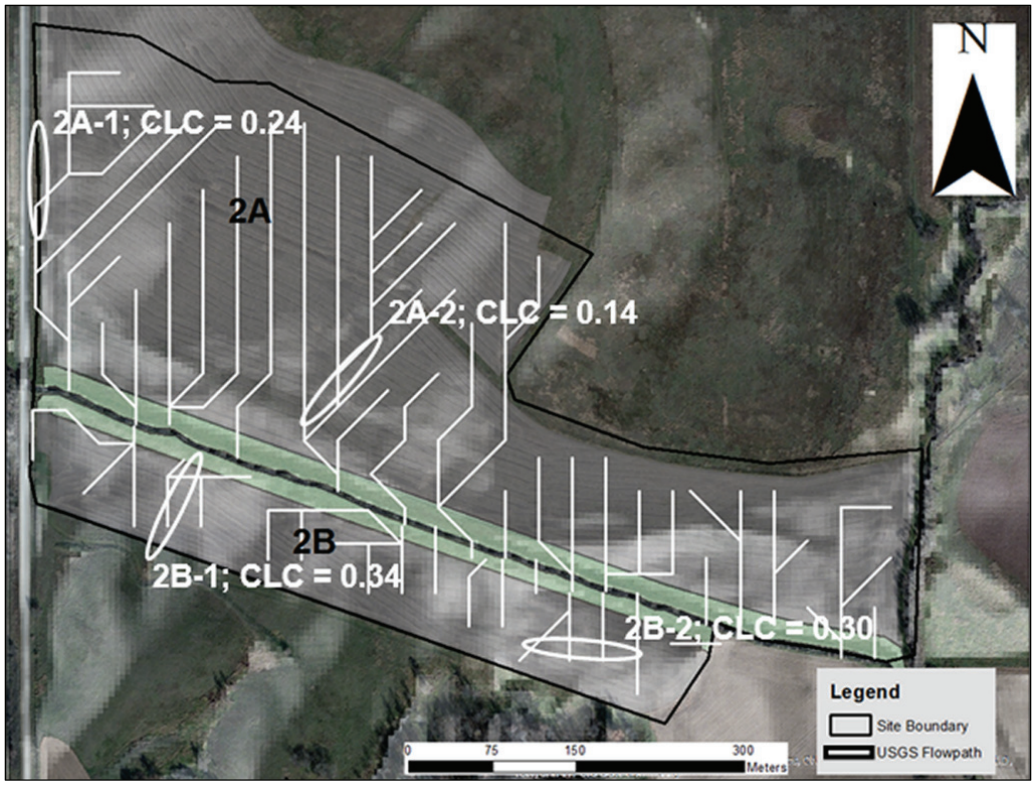

Figure 5. Sub-basin field areas 2A and 2B of site 2 showing USGS 30 m × 30 m DEM-derived flowpaths, observed 100 m flowpath segments (ovals), and coefficients of linear correspondence (CLC) based on geospatial map comparison analysis for Rock Creek watershed in central Iowa.

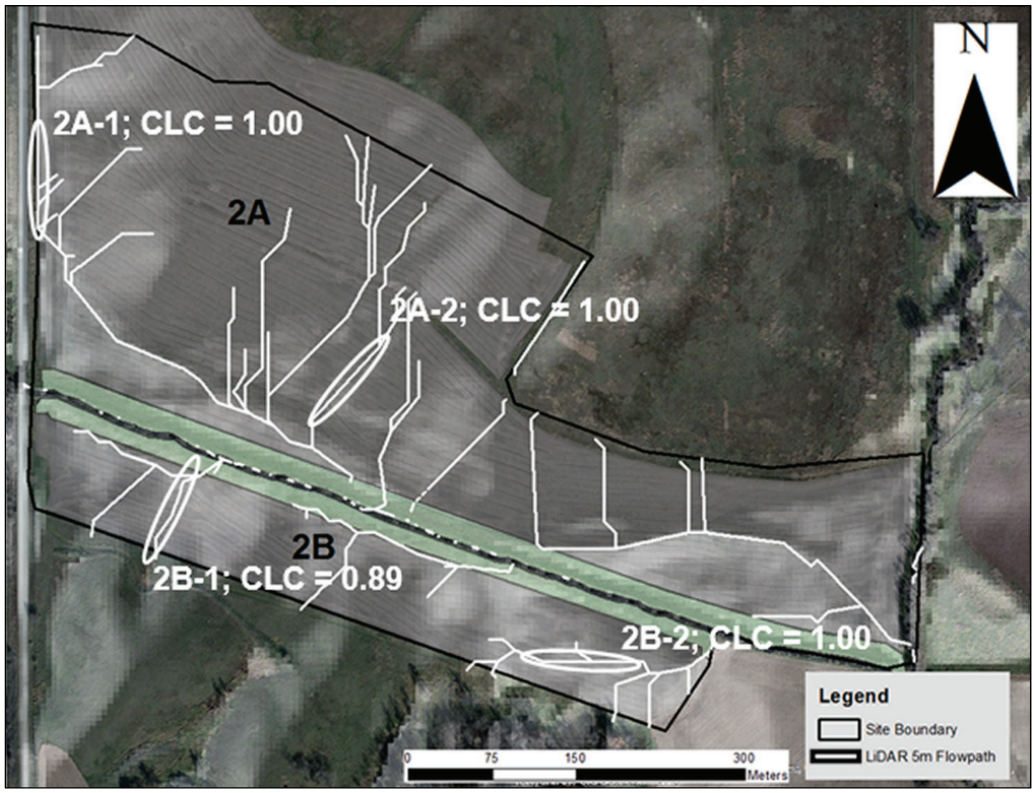

Figure 6. Sub-basin field areas 2A and 2B of site 2 showing LiDAR 5 m × 5 m DEM-derived flowpaths, observed 100 m flowpath segments (ovals), and coefficients of linear correspondence (CLC) based on geospatial map comparison analysis for Rock Creek watershed in central Iowa.

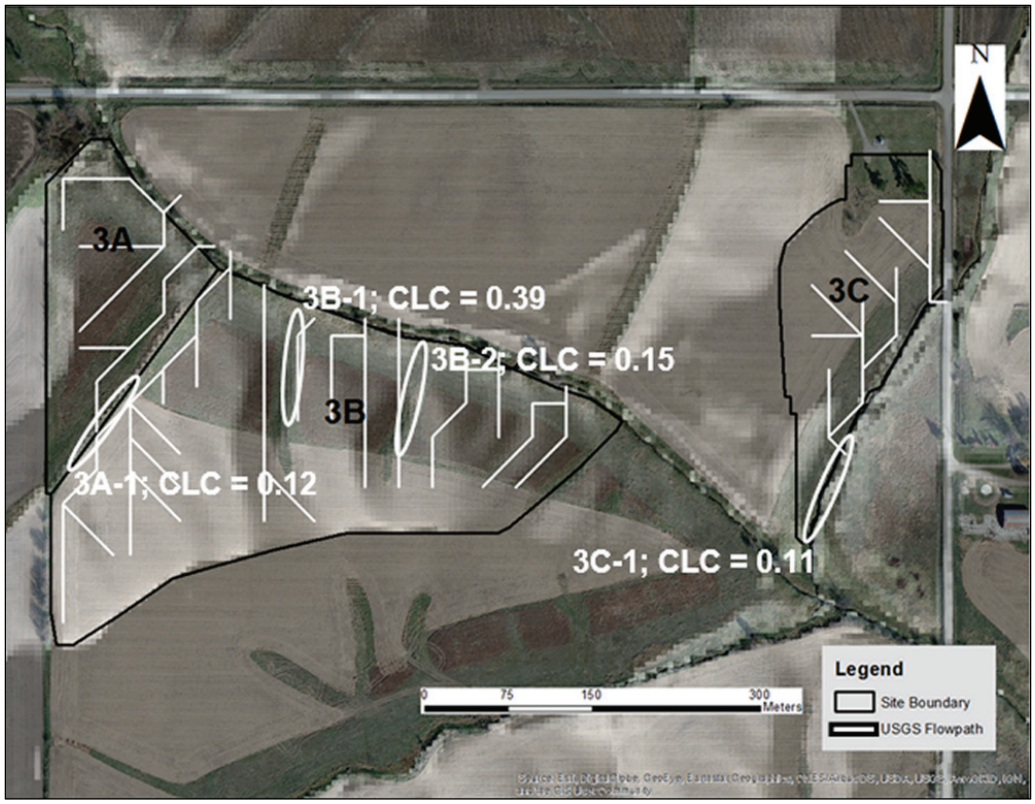

Figure 7. Sub-basin field areas 3A, 3B, and 3C of site 3 showing USGS 30 m × 30 m DEM-derived flowpaths, observed 100 m flowpath segments (ovals), and coefficients of linear correspondence (CLC) based on geospatial map comparison analysis for Rock Creek watershed in central Iowa.

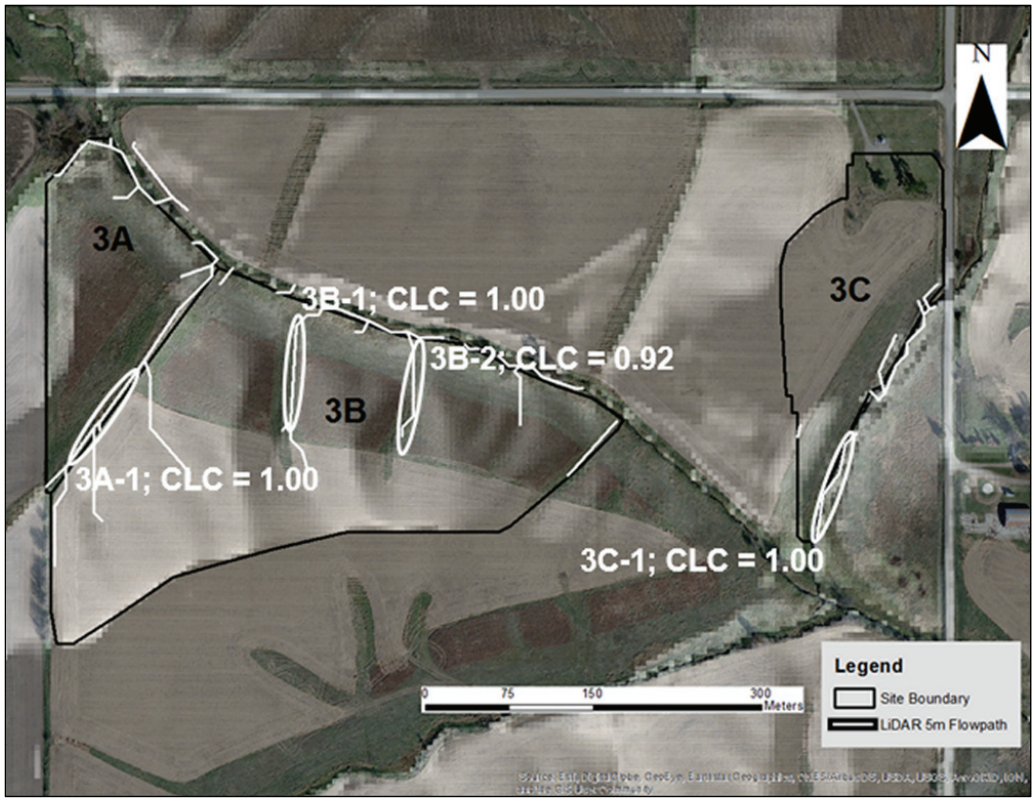

Figure 8. Sub-basin field areas 3A, 3B, and 3C of site 3 showing LiDAR 5 m × 5 m DEM-derived flowpaths, observed 100 m flowpath segments (ovals), and coefficients of linear correspondence (CLC) based on geospatial map comparison analysis for Rock Creek watershed in central Iowa.

conservation BMP areas. Although increasing the crop production area at the expense of established perennial vegetation may seem contrary to what is generally considered good conservation land management, Zreig et al. (2004) determined that VFS buffers wider than 10 m, based on a range of 2 to 15 m, had an insignificant increase in sediment trapping efficiency. Moreover, producers have multiple BMP options that would not remove additional land from production, including cover crops and, for subsurface tile drainage systems, bioreactors and saturated buffers.

Figures 5 and 6 illustrate the hydrologic modeling and geospatial map comparison analysis results for site 2. The oval outlines identify four observed and ground-truthed 100 m flowpath segments and their respective CLC values (2A-1, 2A-2, 2B-1, and 2B-2). The average flowpath lengths (m) and CLC values for the USGS 30 m × 30 m and LiDAR 5 m × 5 m DEMs (table 3) indicate significantly lower ($p \leq 0.05$) lengths for the USGS 30 m × 30 m DEM-derived flowpaths that are within the observed 5 m wide buffered 100 m flowpath segments. Likewise, the results for the LiDAR 5 m × 5 m DEM-derived flowpaths, compared with the observed 5 m buffered 100 m flowpath segments, indicate no significant differences ($p \leq 0.05$) and highly accurate simulated flowpaths.

Similar to the 5 m × 5 m LiDAR DEM-derived flowpaths in site 1 (fig. 4), the simulated flowpaths in site 2 (fig. 6) also show where a slight increase in the riparian VFS buffer width in area 2B would more effectively target the ground-truthed flowpaths that partially bypass the VFS. Additional surface flowpaths in areas 2A and 2B indicate potential target areas where grassed waterways could be applied. Specific targeted flowpaths for grassed waterway application include the oval area in the middle of area 2A and the two oval-outlined flowpaths in area 2B.

Figures 7 and 8 show the hydrologic modeling and geospatial map comparison analysis results for site 3. The oval outlines identify four observed and ground-truthed 100 m flowpath segments and their respective CLC values (3A-1, 3B-1, 3B-2, and 3C-1). Table 3 includes the average flowpath lengths (m) and CLC values for the USGS 30 m × 30 m and LiDAR 5 m × 5 m DEMs. Again, these data indicate that significantly lower ($p \leq 0.05$) lengths were determined for the USGS 30 m × 30 m DEM-derived flowpaths occurring within the observed 5 m wide buffered 100 m flowpath segments. The results for the LiDAR 5 m × 5 m DEM-derived flowpaths, compared with the observed 5 m buffered 100 m flowpath segments, indicate no significant differences ($p \leq 0.05$) and further underscore the hydrologic modeling and simulation accuracy of the high-resolution LiDAR DEM data used in this study.

Compared with the LiDAR 5 m × 5 m DEM-derived flowpaths shown in sites 1 and 2 (figs. 4 and 6), the site 3 map (fig. 8) also shows simulated flowpaths derived from the high-resolution LiDAR DEM data that accurately located several ground-truthed surface flowpath patterns. The patterns in area 3B are associated with runoff-induced soil erosion. However, most of these runoff flowpaths are perpendicular to the stream channel and are not significantly associated with riparian areas, making these flowpaths potential sites for grassed waterway BMP application. Consequently, both the high-resolution LiDAR DEM data and the aerial imagery significantly improve the hydrologic analysis and visualization of site 3 as compared to the USGS DEM data (fig. 7), effectively rendering the position, orientation, and landscape attributes of the surface drainage features. Moreover, the proposed incorporation of these results and procedures into a virtual-reality 3-D decision support tool may further enhance the visualization and hydrologic analysis potential of this remote landscape assessment method.

For the overall statistical analysis of the hydrologic modeling and geospatial map comparison for the three sites in Rock Creek watershed, the LSMEANS values of 19.75 m and 98.42 m are significantly lower ($p \leq 0.05$) and not significantly different ($p \leq 0.05$) for the USGS 30 m × 30 m and LiDAR 5 m × 5 m DEM-derived surface flowpath networks, respectively, as compared to the observed and ground-truthed flowpaths. The LSMEANS results indicated CV values of 67.82 and 3.99 for the USGS and LiDAR DEMs, respectively, further reflecting the accuracy of the LiDAR DEM data at watershed scale. The PBIAS values for sites 1, 2, and 3 (table 4) also reflect the relative accuracy of the USGS 30 m × 30 m and LiDAR 5 m × 5 m DEMs, as indicated by the performance ratings (table 2) of "unsatisfactory" and "very good," respectively.

This study focused primarily on determining the accuracy of DEM-simulated flowpaths relative to observed and ground-truthed flowpaths. These results can be helpful in assessing vegetative BMP design and placement to more effectively intercept surface runoff. However, to fully gauge the performance of a VFS or other similar type of vegetative buffer, it is necessary to include additional hydrologic and terrestrial information, such as the slope of the target area, the extent of normal overland flow versus concentrated flow, the ratio of contributing source area to buffer area, adjacent agricultural cropping systems, local soil types, and vegetation height and species.

Summary and Conclusions

This study sought to quantify the accuracy of simulated surface flowpaths relative to observed and ground-truthed BMP drainage features for more effective placement of vegetative buffers to intercept surface runoff. The research was conducted on three research sites in Rock Creek watershed in central Iowa. Other important factors can also affect vegetative BMP performance, including soil and vegetation type, ratio of contributing source area to buffer area, slope, and concentrated surface flow channels. However, this research focused on using ArcGIS hydrologic modeling and geospatial map comparison analysis to generate simulated surface flowpaths and compare these data with observed and ground-truthed drainage features in the field. The DEM datasets used in this study included internet-available USGS 30 m × 30 m (typically used to site VFS buffers) and LiDAR 5 m × 5 m DEMs.

The results of this study indicated that the LiDAR 5 m × 5 m DEM generated significantly more accurate simulated

surface flowpaths than the USGS 30 m × 30 m DEM and quantitatively demonstrated the efficacy of using high-resolution LiDAR DEM data to more accurately analyze landscape hydrologic conditions, prescribe improvements to existing BMPs, and determine new sites for enhanced BMP placement and functionality. The results also showed qualitatively the locations of surface flowpaths relative to conservation practices and other drainage features in high-resolution aerial imagery.

Although researchers have expressed concerns regarding the computational time required to process high-resolution LiDAR DEM data due to the large file sizes, no significant computational time differences were noted throughout this study using the resampled LiDAR 5 m × 5 m DEM. This may be due in part to the advanced computer systems used, with 16 to 24 GB of processing memory and up to 2 TB of available hard drive capacity. This conclusion was also verified by comparing the file sizes of the USGS 30 m × 30 m and LiDAR 5 m × 5 m DEM datasets used for the research sites via a simple statistical analysis ($p = 0.387$ at 95% probability level [$p \leq 0.05$], indicating no significant differences in file sizes during the study).

This novel approach to displaying quantitative and qualitative surface hydrologic data and imagery can aid NRCS personnel, watershed managers, and landowners in accurately identifying BMP sites. To further explore this approach, the hydrologic data, geospatial map comparison analysis results, and procedures from this study will be applied to multiple watersheds in central Iowa in an effort to develop a cloud-based, user-interactive, virtual-reality DS tool for enhancing field-scale and watershed-scale hydrologic assessment and vegetative BMP design and placement within a high-resolution 3-D imagery environment.

REFERENCES

Arora, K., Mickelson, S. K., & Baker, J. L. (2003). Effectiveness of vegetated buffer strips in reducing pesticide transport in simulated runoff. *Trans. ASAE, 46*(3), 635-644. https://doi.org/10.13031/2013.13599

Arora, K., Mickelson, S. K., Baker, J. L., Tierney, D. P., & Peters, C. J. (1996). Herbicide retention by vegetative buffer strips from runoff under natural rainfall. *Trans. ASAE, 39*(6), 2155-2162. https://doi.org/10.13031/2013.27719

Bansal, M. (2006). Vegetative filter strip assessment in the state of Iowa. MS thesis. Ames, IA: Iowa State University, Department of Agricultural and Biosystems Engineering.

Bater, C. W., & Coops, N. C. (2009). Evaluating error associated with LiDAR-derived DEM interpolation. *Comput. Geosci., 35*(2), 289-300. https://doi.org/10.1016/j.cageo.2008.09.001

Boyd, P. M., Baker, J. L., Mickelson, S. K., & Ahmed, S. I. (2003). Pesticide transport with surface runoff and subsurface drainage through a vegetative filter strip. *Trans. ASAE, 46*(3), 675-684. https://doi.org/10.13031/2013.13602

Broadmeadow, S., & Nisbet, T. R. (2004). The effects of riparian forest management on the freshwater environment: A literature review of best management practice. *Hydrol. Earth Syst. Sci., 8*(3), 286-305. https://doi.org/10.5194/hess-8-286-2004

David, O., Yaege, L., Rojas, K., Green, T., Kipka, H., Lloyd, W., ... Ascough, J. (2014). The Land Management and Operations Database (LMOD). In D. P. Ames, N. W. Quinn, & A. E. Rizzoli (Ed.), *Proc. 7th Intl. Congress Environ. Modeling and Software.* International Environmental Modeling and Software Society. Retrieved from http://www.iemss.org/sites/iemss2014/proceedings.php

Dillaha, T. A., Reneau, R. B., Mostaghimi, S., & Lee, D. (1989). Vegetative filter strips for agricultural nonpoint-source pollution control. *Trans. ASAE, 32*(2), 513-519. https://doi.org/10.13031/2013.31033

Dosskey, M. G., Helmers, M. J., & Eisenhauer, D. E. (2011). A design aid for sizing filter strips using buffer area ratio. *J. Soil Water Cons., 66*(1), 29-39.

Dosskey, M. G., Helmers, M. J., Eisenhauer, D. E., Franti, T. G., & Hoagland, K. D. (2002). Assessment of concentrated flow through riparian buffers. *J. Soil Water Cons., 57*(6), 336-343.

Dosskey, M. G., Hoagland, K. D., & Brandle, J. R. (2007). Change in filter strip performance over ten years. *J. Soil Water Cons., 62*(1), 21-32.

ESRI. (2005). ArcGIS ver. 9.3, ArcView ver. 3.3, and AVSWAT and AVSpatial Analyst extensions. Redlands, CA: Environmental Systems Research Institute.

ESRI. (2014). ArcGIS ver. 10.3. Redlands, CA: Environmental Systems Research Institute.

ESRI. (2016). ArcGIS ver. 10.4. Redlands, CA: Environmental Systems Research Institute.

Gharabhagi, B., Rudra, R. P., Whiteley, H. R., & Dickinson, W. T. (2001). Sediment removal efficiency of vegetative filter strips. ASAE Paper No. 012071. St. Joseph, MI: ASAE.

Goodchild, M. F., & Hunter, G. J. (1997). A simple positional accuracy measure for linear features. *Intl. J. Geogr. Info. Sci., 11*(3), 299-306. https://doi.org/10.1080/136588197242419

Jones, K. L., Poole, G. C., O'Daniel, S. J., Mertes, L. A. K., & Stanford, J. A. (2008). Surface hydrology of low-relief landscapes: Assessing surface water flow impedance using LiDAR-derived digital elevation models. *Remote Sensing Environ., 112*(11), 4148-4158. https://doi.org/10.1016/j.rse.2008.01.024

Lee, K.-H., Isenhart, T. M., & Schultz, R. C. (2003). Sediment and nutrient removal in an established multi-species riparian buffer. *J. Soil Water Cons., 58*(1), 1-8.

Li, J., & Wong, D. W. S. (2010). Effects of DEM sources on hydrologic applications. *Comput. Environ. Urban Syst., 34*(3), 251-261. https://doi.org/10.1016/j.compenvurbsys.2009.11.002

Li, S., MacMillan, R. A., Lobb, D. A., McConkey, B. G., Moulin, A., & Fraser, W. R. (2011). LiDAR DEM error analyses and topographic depression identification in a hummocky landscape in the prairie region of Canada. *Geomorphology, 129*(3), 263-275. https://doi.org/10.1016/j.geomorph.2011.02.020

Liu, X. (2008). Airborne LiDAR for DEM generation: Some critical issues. *Prog. Phys. Geogr., 32*(1), 31-49. https://doi.org/10.1177/0309133308089496

Magellan. (2004). SporTrak and Explorist 200 handheld GPS units. Santa Clara, CA: Magellan Navigation, Inc. Retrieved from www.magellangps.com

Meyer, L. D., Dabney, S. M., & Harmon, W. C. (1995). Sediment-trapping effectiveness of stiff-grass hedges. *Trans. ASAE, 38*(3), 809-815. https://doi.org/10.13031/2013.27895

Minnick, R. F. (1964). A method for the measurement of areal correspondence. *Papers of the Michigan Academy of Science, Arts, and Letters, 49*, 333-334.

Moriasi, D. N., Arnold, J. G., Van Liew, M. W., Bingner, R. L., Harmel, R. D., & Veith, T. L. (2007). Model evaluation guidelines for systematic quantification of accuracy in watershed simulations. *Trans. ASABE, 50*(3), 885-900. https://doi.org/10.13031/2013.23153

Murphy, P. N. C., Ogilvie, J., Meng, F.-R., & Arp, P. (2008). Stream network modelling using LiDAR and photogrammetric digital elevation models: A comparison and field verification.

Hydrol. Proc., 22(12), 1747-1754. https://doi.org/10.1002/hyp.6770
Neibling, W. H., & Alberts, E. E. (1979). Composition and yield of soil particles transported through sod strips. ASAE Paper No. 792065. St. Joseph, MI: ASAE.
Nestrud, L. M., & Worster, J. R. (1979). Soil survey of Jasper County, Iowa. Washington, DC: USDA Soil Conservation Service.
NSSDA. (1998). Geospatial positioning accuracy standards, Part 3: National standard for spatial data accuracy. FGDC-STD-007.3-1998. Reston, VA: U.S. Geological Survey, Federal Geographic Data Committee.
Ree, W. O. (1949). Hydraulic characteristics of vegetation for vegetated waterways. *Agric. Eng., 80*(4), 184-189.
Richardson, M. S., & Gatti, R. C. (1999). Prioritizing wetland restoration activity within a Wisconsin watershed using GIS modeling. *J. Soil Water Cons., 54*(3), 537-542.
SAS. (2016). *SAS user's guide: Statistics*. Ver. 9.4. Cary, NC: SAS Institute, Inc.
Shrivastav, M. (2015). Using ArcGIS hydrologic modeling and LiDAR digital elevation data to evaluate surface runoff interception performance of riparian vegetative filter strip buffers in central Iowa. MS thesis. Ames, IA: Iowa State University, Department of Agricultural and Biosystems Engineering.
Starks, P. J., & Moriasi, D. N. (2017). Impact of eastern redcedar encroachment on stream discharge in the North Canadian River basin. *J. Soil Water Cons., 72*(1), 12-25. https://doi.org/10.2489/jswc.72.1.12
Subra, W., & Waters, J. (1996). Nonpoint-source pollution. *Proc. Intl. Symp. on Geoscience and Remote Sensing* (vol. 4, pp. 2231-2233). Piscataway, NJ: IEEE. Retrieved from http://ieeexplore.ieee.org/document/516945/
Trimble. (2005). Trimble 5800-R8 handheld GPS unit. Dayton, OH: Trimble Navigation Ltd. Retrieved from www.trimble.com
Unwin, D. J. (1981). *Introductory spatial analysis*. London, UK: Methuen.
USEPA. (2000). Atlas of America's polluted waters. EPA 840-B00-002. Washington, DC: U.S. Environmental Protection Agency.
USEPA. (2009). National water quality inventory: Report to Congress, 2004 reporting cycle. EPA 841-R-08-001. Washington, DC: U.S. Environmental Protection Agency.
USEPA. (2012). Clean Water Act and pollutant total maximum daily loads (TMDLs). Congressional Research Service Report No. R42752. Washington, DC: U.S. Environmental Protection Agency.
USGS. (2010). The quality of our nation's water: Nutrients in the nation's streams and groundwater, 1992-2004. USGS Circular 1350. Reston, VA: U.S. Geological Survey.
Van Dijk, P. M., Kwaad, F. J. P. M., & Klapwijk, M. (1996). Retention of water and sediment by grass strips. *Hydrol. Proc., 10*(8), 1069-1080. https://doi.org/10.1002/(SICI)1099-1085(199608)10:8<1069::AID-HYP412>3.0.CO;2-4
Vaze, J., Teng, J., & Spencer, G. (2010). Impact of DEM accuracy and resolution on topographic indices. *Environ. Model. Softw., 25*(10), 1086-1098. https://doi.org/10.1016/j.envsoft.2010.03.014
Wang, X., & Yin, Z.-Y. (1998). A comparison of drainage networks derived from digital elevation models at two scales. *J. Hydrol., 210*(1), 221-241. https://doi.org/10.1016/S0022-1694(98)00189-9
Webber, D. F. (2000). Comparing estimated surface flowpaths and sub-basins derived from digital elevation models (DEMs) of Bear Creek watershed in central Iowa. MS thesis. Ames, IA: Iowa State University, Department of Agricultural and Biosystems Engineering.
Webber, D. F., Mickelson, S. K., Richard, T. L., & Ahn, H. K. (2009). Effects of a livestock manure windrow composting site with a fly ash pad surface and vegetative filter strip buffers on sediment, nitrate, and phosphorus losses with runoff. *J. Soil Water Cons., 64*(2), 163-171. https://doi.org/10.2489/jswc.64.2.163
Webber, D. F., Mickelson, S. K., Ahmed, S. I., Russell, J. R., Powers, W. J., Schultz, R. C., & Kovar, J. L. (2010a). Livestock grazing and vegetative filter strip buffer effects on runoff sediment, nitrate, and phosphorus losses. *J. Soil Water Cons., 65*(1), 34-41. https://doi.org/10.2489/jswc.65.1.34
Webber, D. F., Mickelson, S. K., Wulf, L. W., Richard, T. L., & Ahn, H. K. (2010b). Hydrologic modeling of runoff from a livestock manure windrow composting site with a fly ash pad surface and vegetative filter strip buffers. *J. Soil Water Cons., 65*(4), 252-260. https://doi.org/10.2489/jswc.65.4.252
Wehr, A., & Lohr, U. (1999). Airborne laser scanning: An introduction and overview. *ISPRS J. Photogram. Remote Sensing, 54*(2), 68-82. https://doi.org/10.1016/S0924-2716(99)00011-8
Wenger, S. (1999). A review of the scientific literature on riparian buffer width, extent, and vegetation. Athens, GA: University of Georgia, Institute of Ecology.
Zhang, H., & Huang, G. (2009). Building channel networks for flat regions in digital elevation models. *Hydrol. Proc., 23*(20), 2879-2887. https://doi.org/10.1002/hyp.7378
Zhao, Z., Benoy, G., Chow, T. L., Rees, H. W., Daigle, J.-L., & Meng, F.-R. (2010). Impacts of accuracy and resolution of conventional and LiDAR based DEMs on parameters used in hydrologic modeling. *Water Resour. Mgmt., 24*(7), 1363-1380. https://doi.org/10.1007/s11269-009-9503-5
Zreig, M. A. (2001). Factors affecting sediment trapping in vegetated filter strips: Simulation study using VFSMOD. *Hydrol. Proc., 15*(8), 1477-1488. https://doi.org/10.1002/hyp.220
Zreig, M. A., Rudra, R. P., Lalonde, M. N., Whiteley, H. R., & Kaushik, N. K. (2004). Experimental investigation of runoff reduction and sediment removal by vegetated filter strips. *Hydrol. Proc., 18*(11), 2029-2037. https://doi.org/10.1002/hyp.1400

NOMENCLATURE

ANOVA = analysis of variance
BMP = best management practice
CAC = coefficient of areal correspondence
CLC = coefficient of linear correspondence
CV = coefficient of variation
CWA = Clean Water Act
DEM = digital elevation model
DS = decision support
GB = gigabyte
GIS = geographical information system
GLM = general linear model
GPS = global positioning system
LiDAR = light detection and ranging
LSMEANS = least square means
NED = National Elevation Dataset
NPS = nonpoint-source
PBIAS = percent bias
TB = terabyte
VFS = vegetative filter strip